Sensors and Materials, Vol. 10, No. 2 (1998) 093–102
MYU Tokyo

S & M 0316

Air/Fuel Sensors Based on Pt- and TiO_2-Doped Nb_2O_5 Film

Zhu Jianzhong, Ren Congxin, Chen Guoliang,
Mu Haichuan, Wu Jiali and Yu Chunying[1]

State Key Laboratories of Transducer Technology, Shanghai Institute of Metallurgy,
Chinese Academy of Sciences, Shanghai 200050, China
[1]Dalian Institute of Chemical Physics, Chinese Academy of Sciences, Dalian 116023, China

(Received October 11, 1996; accepted December 1, 1997)

Key words: air/fuel sensors, metal oxide semiconductor, ion-beam-enhanced deposition

In this paper we describe the preparation of TiO_2-doped Nb_2O_5 thin film using the ion-beam-enhanced deposition (IBED) technique, and the development of a new automobile air/fuel (A/F) sensor with an additionally integrated platinum temperature sensor and a Pt heater. The resistive jump at the stoichiometric point in the characteristic curve is three orders of magnitude. The response time of the sensor is 10 and 100 ms when the atmosphere is changed from λ = 0.9 to 1.1 and vice versa, respectively. The sensor performance stabilized after 7 measurements. Preliminary results indicate that this sensor has the potential to monitor the λ value of automobile exhaust gas.

1. Introduction

In view of the increasingly strict regulations for emissions from motor vehicles and heating systems, the need for modern, cost-effective and reliable sensors to measure the λ value during combustion has become urgent. In addition to conventional sensors based on the oxygen-ion conductor ZrO_2, sensors fabricated using semiconducting oxygen-sensitive metal oxide thin and thick films such as TiO_2,[1] Nb_2O_5,[2] $SrTiO_3$,[3] CeO_2,[4] Ga_2O_3,[5] $SrSnO_3$,[6] and TiO_2-doped Nb_2O_5,[7] represent the most promising sensors for future applications. They offer the potential to measure the resistive jump at the stoichiometric point in the characteristic curve as well as the λ value, even in the case of $\lambda \neq 1$. For example, air/fuel mixtures are combusted at $\lambda = 1 \pm 0.01$ in internal combustion engines using the regulated three-way catalyst case, at $\lambda = 1.3 - 1.7$ in lean-burning engines, and at

$\lambda = 1.1 - 1.3$ in heat-producing burners. Moreover, this new type of sensor opens up the possibility of cost-effective production due to the implementation of planar microsystem technology.

Some oxygen-sensitive materials such as $SrTiO_3$ show p-type and n-type conductivities that depend on the values of the partial pressure of oxygen. This leads to ambiguous response of the sensors in specific applications; however, but the ambiguity can be avoided by the selective incorporation of dopants. A doped sensor with a low acceptor concentration results in reduction of response time and improvement of selectivity, as well as an increase in oxygen sensitivity and temperature stability. There are only a few reports that describe the doping processes. In this study, an ion-beam-enhanced deposition (IBED) technique was used to incorporate dopants in thin films as precisely as possible. IBED, in which atom deposition and ion bombardment take place simultaneously on the surface of the specimen, is one of the newest techniques for film formation. It has many advantages such as improved film adhesion to the substrate, accurately controlled composition and thickness of the film, and easy syntheses of compound films at low temperatures. In addition to describing this technique, the characteristics of the sensor are also discussed in detail in this paper.

2. Experimental

Using the IBED technique and microelectron planar technology, automotive A/F sensors were produced on Al_2O_3 substrates consisting of an oxygen-sensitive TiO_2-doped Nb_2O_5 element, a platinum temperature sensor and a Pt heater (see Fig. 1).

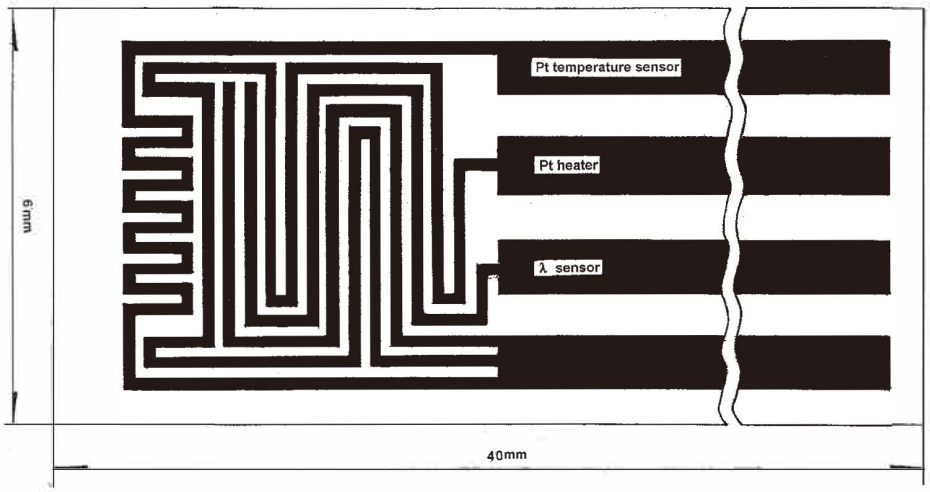

Fig. 1. The structure of the λ-sensors.

A Pt thin film of 1 μm thickness was deposited by IBED, and was patterned using the conventional lift-off photolithographic process.

The TiO_2-doped Nb_2O_5 thin film was deposited on a cooled Al_2O_3 substrate by IBED using a single ion source with Ar ions from a combined target of TiO_2 and Nb_2O_5 (purity concentration 5×10^{-3}% w/w). The amount of TiO_2 dopant in Nb_2O_5 could be changed by changing the area ratio of TiO_2 to Nb_2O_5 target (see Fig. 2). The doping dose of TiO_2 in Nb_2O_5 could also be accurately adjusted by varying IBED parameters such as ion beam energy, ion beam current density and angle of incidence. The patterns of the Nb_2O_5 thin film were delineated using the lift-off technique. During deposition, the total pressure in the operation chamber of the sputtering system was approximately 1.6×10^{-2} Pa using 66.7% Ar and 33.3% O_2. The average sputtering power was approximately 2 W/cm^2, which resulted in a deposition rate of 24 nm/min. Films with thickness between 0.5 and 1.5 μm were then tempered in air for 2 h at 1000°C to obtain a structure that was stable under high temperatures. The films were investigated by electrical measurements, X-ray diffraction (XRD), infrared spectrometry (IRS) and scanning electron microscopy (SEM). Analysis of the amount of TiO_2 dopant was carried out using inductively coupled plasma atomic emission spectrometry (ICP-AES). The dependence of the electrical resistance of the TiO_2-doped Nb_2O_5 thin film on temperature was measured using a quartz vessel in a tube furnace either in the presence of nitrogen or oxygen. The R-T characteristic of the specimen was measured in the presence of the exhaust gas from an oxygen-propane combustion in the temperature range of 550 to 750°C. Propane, oxygen and nitrogen were

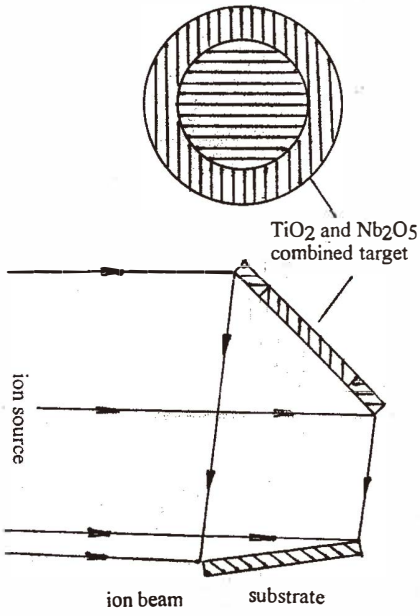

Fig. 2. Principle of doping and simultaneous deposition in the IBED system.

mixed in appropriate ratios to obtain the desired λ value, then the gas mixture was burned at 450°C over a combustive catalytic case. The exhaust gas was introduced into the quartz vessel in which an yttria-stabilized zirconia (YSZ) oxygen sensor was installed to monitor the equilibrium partial pressure of oxygen. The resistance of the specimen was measured using a 8840A multimeter. Figure 3 shows the schematic diagram of the measurement system of the sensors.

3. Results and Discussion

3.1 *Characteristic factor and activation energy*

It is common knowledge that the electrical resistance of metal oxide semiconductor film depends on P_{O_2} according to the following equation:

$$R = R_0 \exp(E / kT)\left(P_{O_2}\right)^{1/m}, \tag{1}$$

where m is a characteristic factor that serves as a measure of the sensitivity to oxygen, E the activation energy, k the Boltzmann constant, T the substrate temperature and P_{O_2} the partial oxygen pressure. For two different partial oxygen pressures P_1 and P_2 at a fixed temperature, we have

$$R_1/R_2 = \left(P_1/P_2\right)^{1/m}.$$

Therefore,

$$m = \log\left(P_1/P_2\right)/\log\left(R_1/R_2\right).$$

For two different temperatures T_1 and T_2 at a constant pressure, we obtain

$$R_1'/R_2' = \exp\left[E\left(\frac{1}{kT_1} - \frac{1}{kT_2}\right)\right],$$

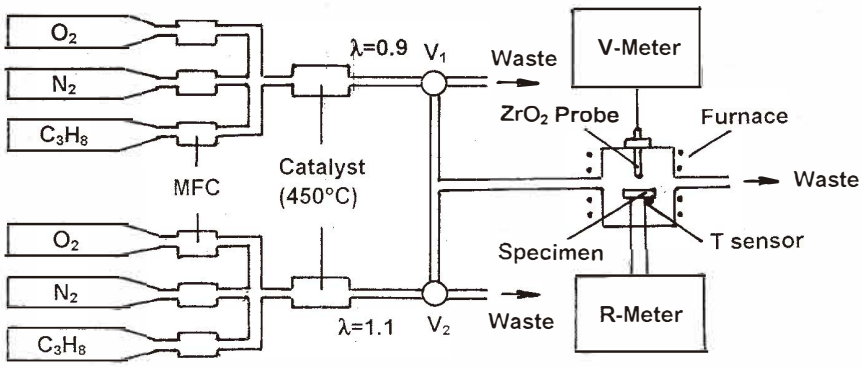

Fig. 3. Schematic diagram of the measurement system of the sensors.

hence,

$$E = k \log\left(R_1' / R_2'\right) \Big/ \left(\frac{1}{T_1} - \frac{1}{T_2}\right) \qquad (c = 1.6 \times 10^{-12}).$$

The measured data of the resistance of TiO_2-doped Nb_2O_5 thin film ($TiO_2/(TiO_2 + Nb_2O_5) = 75$ mol%) and the calculated m values are listed in Table 1.

The characteristic factor m, the activation energy E and the constant R_o of the films for various mol% of TiO_2 to Nb_2O_5 are listed in Table 2.

The preliminary results shown in Table 2 indicate that the characteristic factor m decreased, i.e., the sensitivity to oxygen increased and the activation energy E decreased, so that the effect of temperature on the resistance of the film decreased as the ratio of TiO_2 to Nb_2O_5 was decreased. Thus, we chose 5 mol% TiO_2 to Nb_2O_5 as the film composition for the remaining experiments.

The dependence of the characteristic factor m on the ratio of TiO_2 to Nb_2O_5 is similar to that found by Ohtak *et al.*[7]

3.2 *Resistance-λ characteristic curve*

The resistance-λ characteristic curves at different temperatures are shown in Fig. 4. The jump in the curves at the stoichiometric point is greater than 3 orders of magnitude. The effect of temperature on the resistance of the sensor is greater in the lean-burning

Table 1
Dependence of sensor resistance on the partial pressure of oxygen at 700°C and the calculated m values.

Atmosphere	P_{O2} (kPa)	R (kΩ)	m	$\overline{m}$
O_2	100	1050	4.896	
N_2	0.01	160	4.896	
O_2	100	1010	4.880	4.9
N_2	0.01	153	4.880	
O_2	100	963	4.918	
N_2	0.01	148	4.918	

Table 2
Dependence of m, E and R_o of the film on the ratio of TiO_2 to Nb_2O_5.

$TiO_2/(TiO_2+Nb_2O_5)$ (mol%)	m	E (eV)	R_o (Ω)
75	4.9	0.74	0.24
25	4.9	0.20	4030
5	4.3	0.10	4467

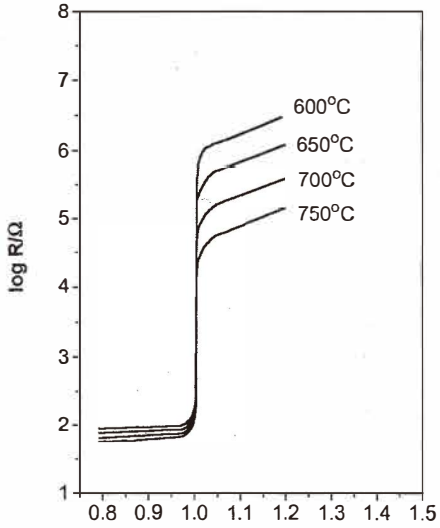

Fig. 4. Resistance-λ characteristic curve of the λ-sensor at different temperatures.

region than in the rich-burning region in the temperature range of 600 to 750°C. Hence, the resistance jump of the sensor at low temperatures is larger than that at high temperatures. Figure 5 shows that the resistance-λ curve in the λ range of 1.1–1.6 is almost linear. Although the slope is small, the λ sensor offers the potential to measure λ from 1.3 to 1.7 in lean-burning engines.

3.3 *Response time*

It is well known that the ratio of diffusion coefficient to mobility for a charged particle is subject to Einstein's relational expression:

$$\frac{D}{\mu} = \frac{kT}{q}, \tag{2}$$

where D is the diffusion coefficient, μ the mobility of the charged particle, q the charge of the particle, k the Boltzmann constant and T the substrate temperature (K).

Considering the contribution of both electron and oxygen vacancies to mobility, one obtains:[4]

$$\mu = \frac{\mu_e \cdot \mu_v}{\mu_e + \mu_v}, \tag{3}$$

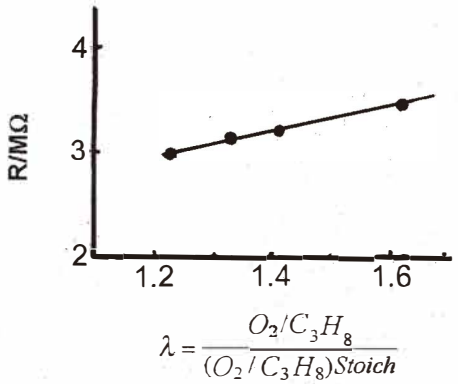

Fig. 5. Resistance-λ curve in the range of λ =1.1–1.6 at 750°C.

$$\mu_e = 0.036 \exp\left(-\frac{E_h}{kT}\right), \tag{4}$$

$$\mu_v = \frac{346}{T} \exp\left(-\frac{E_v}{kT}\right), \tag{5}$$

where E_h = 0.15 eV and E_v = 0.84 eV are hopping energies for electron and oxygen vacancies, respectively.

For a bivalent oxygen vacancy, the formula for the diffusion coefficient can be written as

$$D = \frac{kT}{2e}\mu \cong 0.0149 \exp\left(-\frac{9739}{T}\right). \tag{6}$$

Therefore, the response time is given as follows:

$$\chi_0 = D\tau, \tag{7}$$

$$\tau = \chi_0^2 / D \cong 67.1\chi_0^2 \exp\left(\frac{9739}{T}\right), \tag{8}$$

where χ_0 is the diffusion length, and τ the response time. If χ_0 =1.0 μm and T = 973 K, then $\tau \cong$ 15 ms. This is only a theoretical estimation. It tells us how high the level of response time is for solid thin-film sensors. In this study, the response time of the sensor depends not only on the temperature of the substrate and the thickness of the sensitive film (diffusion within a solid), but also on various factors including gas diffusion, absorption, reaction and porous diffusion as well as on the gas species of environment and the catalyst in the film. There were no significant differences in the response time between the sensor without the

Pt catalyst and that with Pt when the atmosphere was changed between nitrogen and oxygen and between propane and oxygen. It took 3.5 min to establish a stable response when the atmosphere was changed from nitrogen to oxygen (Fig. 6). However, the response time of the sensor was shorter than 0.1 min when the atmosphere was changed from propane to oxygen (Fig. 7). When the atmosphere was changed from λ =1.1 to 0.9, the response time of the sensor with Pt was shorter than that of the sensor without Pt (Fig. 8). Compared with the response time of the ZrO_2 oxygen sensor (20 ms; LSH 23 Bosch, Germany), that of the Nb_2O_5 film sensor (10 ms) was shorter when the atmosphere was changed from λ = 0.9 to 1.1. These times contrast those when λ =1.1 to 0.9 (100 ms and 20 ms, respectively) (Fig. 9).

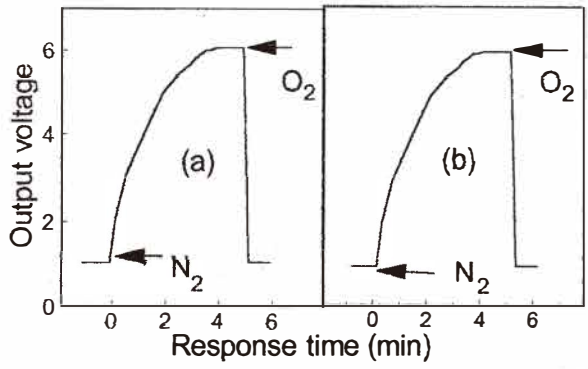

Fig. 6. Response curves for the sensors without Pt (a) and with Pt (b) at 750°C when the atmosphere was changed from nitrogen to oxygen and vice versa.

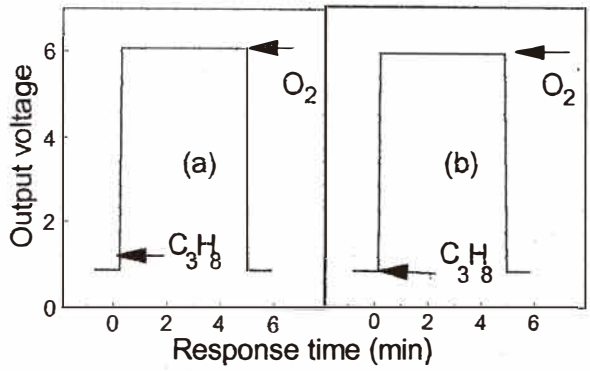

Fig. 7. Response curves for the sensors without Pt (a) and with Pt (b) at 750°C when the atmosphere was changed from propane to oxygen and vice versa.

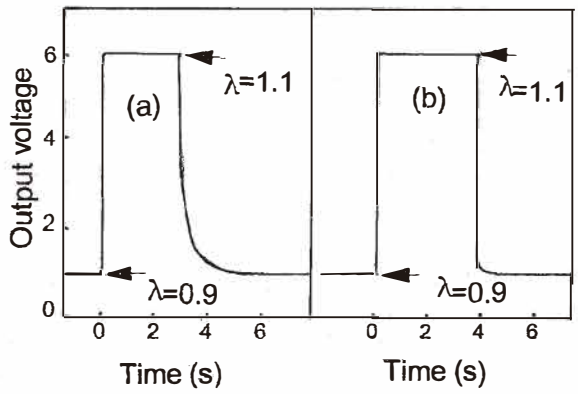

Fig. 8. Response curves for the sensors without Pt (a) and with Pt (b) at 600°C when λ was changed from 0.9 to 1.1 and vice versa.

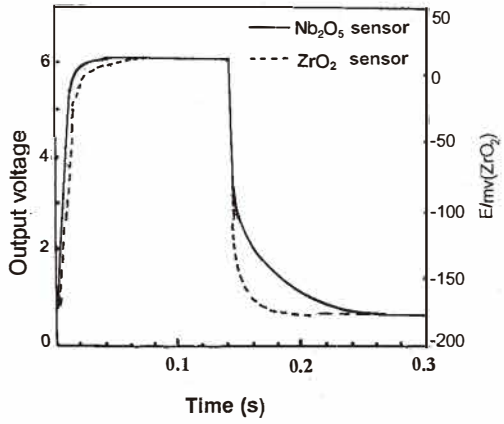

Fig. 9. Comparison between the response time for the Nb_2O_5 sensor and that for the ZrO_2 oxygen sensor at 600°C when λ was changed from 0.9 to 1.1 and vice versa.

3.4 *Stability*

Equation (1) shows that the lower the activation energy, the lower the TCR (temperature coefficient of resistance) for oxygen-sensitive films; that is, the thermostability of the oxygen-sensitive device is higher. Figure 10 shows the stability of the λ-sensor. Initially the λ-sensor exhibited high sensitivity that decreased slightly as the measurement time increased; it became stable after seven measurements were taken. Therefore, to carry out the aging process, the stable response characteristic of the sensors must be obtained.

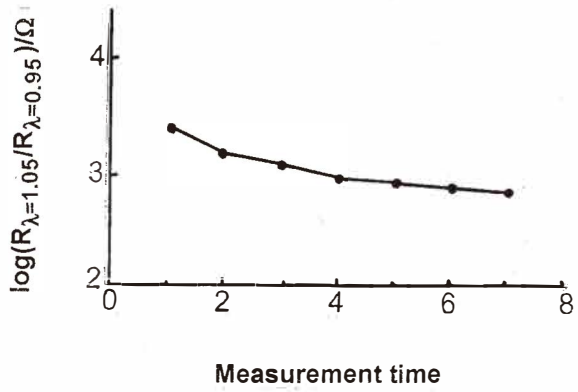

Fig. 10. Resistance jump at the stoichiometric point in the characteristic curves, which changes with the measurement time.

4. Conclusion

A new automotive air/fuel sensor based on TiO_2-doped Nb_2O_5 thin film was developed using the IBED technique and planar microsystem technology. The sensor performed well, exhibiting such factors as high sensitivity and good stability, as well as the possibility of cost-effective production. However, further studies are needed to produce a λ-sensor with optimum performance that can be applied to automotives. For example, it is necessary to place a protective layer on the surface of oxygen-sensitive films to reduce adverse effects, specifically those due to the toxicity of lead, sulfur and phosphorus.

Acknowledgment

The authors gratefully acknowledge financial support from Ford and NSFC, the State Key Laboratory of Transducer Technology and the Ion Beam Laboratory of the Chinese Academy of Sciences.

References

1 E. M. Logothetis: Automotive Oxygen Sensor, Chemical Sensor Technology, Vol. 3 ed. N. Yamazoe (Kodanasha, Tokyo/Elsevier, Amsterdam, 1991) 89.
2 H. Kondo, H. Takahashi, T. Takeuchi and I. Igarashi: Proc. 3rd Sensor Symp. (Japan, 1983) 185.
3 H. Meixner, J. Gerblinger and M. Fleischer: Sensors and Actuators B **15–16** (1993) 45.
4 H. J. Beie and A. Gnorich: Sensors and Actuators B **4** (1991) 393.
5 U. Lampe, M. Fleischer and H. Meixner: Sensors and Actuators B **17** (1994) 187.
6 C. Y. Yu, Y. X. Chen and W. Z. Li: Chemical Sensors (in Chinese) **11** (1991) 43.
7 M. Ohtak, J. Peng, K. Eguchi and H. Arai: Sensors and Actuators B **13–14** (1993) 495.